Heat Treat 2019: Proceedings of the
30th ASM Heat Treating Society Conference
October 15–17, 2019, Detroit, Michigan, USA

Causes of Distortion during High Pressure Gas Quenching Process of Steel Parts

Justin Sims, Zhichao (Charlie) Li, B. Lynn Ferguson
DANTE Solutions, Inc., Cleveland, OH, U.S.A.

Abstract

Quench hardening is a necessary process for improving the mechanical and fatigue performance of load bearing steel components, but liquid quenching can lead to large distortions. High pressure gas quenching is becoming a more popular choice, with the assumption that a slower cooling rate will lead to less distortion. While true for certain geometries, nonlinearities in distortion response can make understanding the dimensional change of a component difficult due to the inherently complex behavior during quenching. Through the use of modeling, and a specially designed coupon, the out-of-round distortion of an eccentric bore is examined for common high-pressure gas quenching conditions. The causes of distortion are examined and explained using the model, with insights into why the cooling rate has a nonlinear relation with distortion.

Introduction

High pressure gas quenching (HPGQ) is touted as a means to reduce distortion of difficult to quench geometries. Quench pressures and quench gas flow velocities are chosen to impart the slowest cooling rate, while still achieving the desired mechanical properties. While it is true that HPGQ imparts a more uniform method of heat extraction when compared to liquid quenching [1-2], due to convective cooling only, that does not necessarily mean less distortion of the component. However, a more uniform quench can result in more consistent distortion. Liquid quenching can lead to inconsistent results due to the chaotic nature of the vapor blanket and the unpredictability of the vapor blanket's degradation into nucleate boiling [2]. Uniformity in this instance is in reference to the heat transfer coefficient witnessed by the surface of the component, not the heat flux through the surface. The heat flux out of the part is a combination of the heat transfer coefficient and the component geometry.

Assuming this heat transfer coefficient can be made perfectly uniform on all surfaces, geometric features will still create nonuniform cooling scenarios [3]. These nonuniform cooling conditions can create nonlinearities in the distortion response of certain geometries. This paper will explore one such geometric feature: An eccentric bore. Such a feature should immediately stand out as a difficult to quench geometry due to the non-balanced mass distribution. Not only is the distortion of this geometry difficult to control, the nonlinear distortion response to different heat transfer coefficients makes selection of proper gas quenching parameters non-intuitive.

Finite Element Model Description

Geometry and Finite Element Model

The study utilized a 50.8 mm thick, 101.6 mm diameter disk, with a 50.8 mm eccentric bore, as shown in Fig. 1. The thinnest cross-section measures 6.35 mm. The thickest cross-section measures 44.45 mm. The geometry was chosen for the nonuniform heating/cooling which occurs due to the nonsymmetric mass distribution.

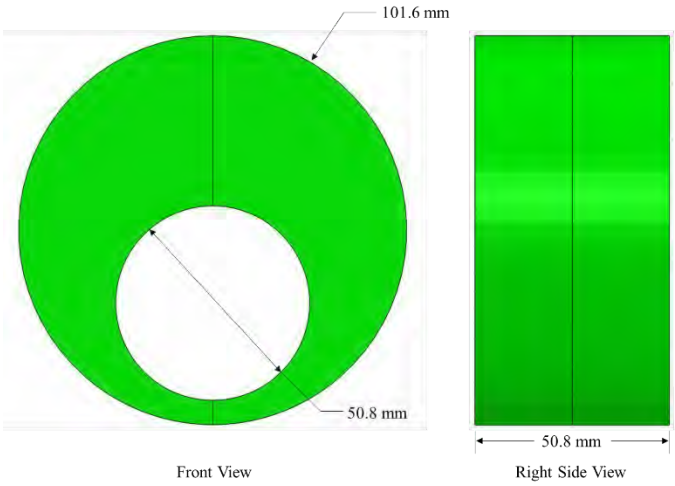

Figure 1: Model geometry, with dimensions, used for study.

Taking advantage of symmetry, the model was reduced to a quarter section, as shown in Fig. 2. This reduction is possible if the heat transfer coefficient applied to the surface is uniform on all surfaces. In keeping the study limited to the geometry's effect on distortion, this is a valid assumption. All nodes on the YZ-Plane Symmetry surface, shown in Fig. 2(B), cannot translate in the x-direction and all nodes on the XY-Plane Symmetry cannot translate in the z-direction.

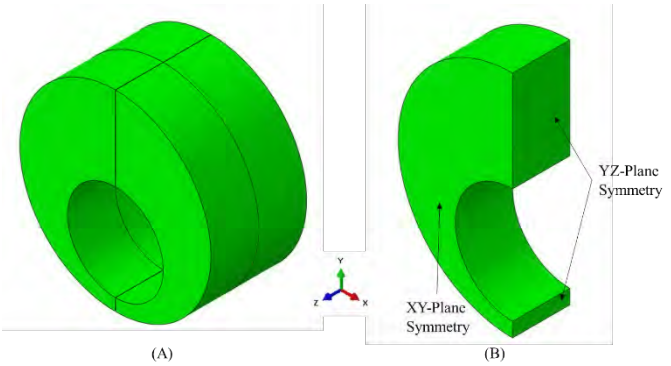

Figure 2: (A) Full, 3D model of geometry and (B) Quarter model used for study.

The 3-dimensional solid model of the quarter section geometry was then meshed in Abaqus for finite element analysis (FEA). Abaqus Standard was used as the FE solver, and DANTE was used to predict the material's response during heat treatment. Figure 3 shows the quarter model properly meshed for heat treatment simulation. Figure 3(A) shows the fine mesh near all surfaces which would be exposed to the atmosphere. Figure 3(B) shows a close-up of the mesh near a corner. The fine mesh near the surface is required to properly describe the steep temperature and phase transformation gradients that occur from the surface towards the core during the heat treating process.

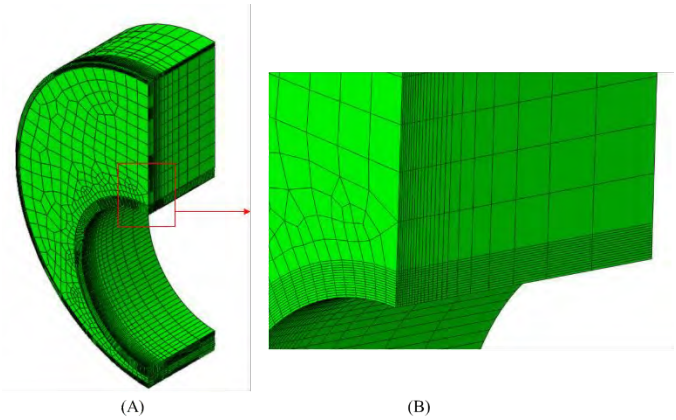

Figure 3: (A) Mesh used for quarter model and (B) Close-up of surface mesh.

Process Description

The study examined a range of heat transfer coefficients (HTC) typical of HPGQ and the distortion response of the coupon shown in Fig. 1 made from Ferrium® C64™. The chemical composition of Ferrium C64 is shown in Table 1.

Table 1: Chemical composition of Ferrium C64.

Ferrium® C64™ Chemical Composition (nominal wt. %)

Fe	C	Co	Cr	Ni	Mo	W	V
Bal.	0.11	16.3	3.5	7.5	1.75	0.2	0.02

Each quench vessel, whether for gas or liquid quenching, will behave differently, with respect to the heat transfer coefficient realized by the component. The chamber pressure and quenchant velocity over the part are two of the most critical parameters when determining a proper HTC to describe a HPGQ vessel. While local variations in the heat transfer coefficient can exist due to effects from component geometry or vessel flow characteristics, generally a constant HTC can be used to describe a HPGQ process. As such, this study ignored any HTC nonuniformities. However, unlike liquid quenchants, gas quenchants experience a fluctuation in ambient temperature near the part.

Figure 4 shows the ambient gas temperature as a function of time used for the modeling study. The curve describes a dual chamber system, whereas the single component, or small load, is heated in one chamber under vacuum or a protective atmosphere, transferred in a vacuum chamber, and loaded into a pressure vessel at room temperature. The ambient gas temperature in the vessel rapidly increases as the hot load is introduced, then cools as the heat exchanger continually cools the quench gas, reducing the component's temperature.

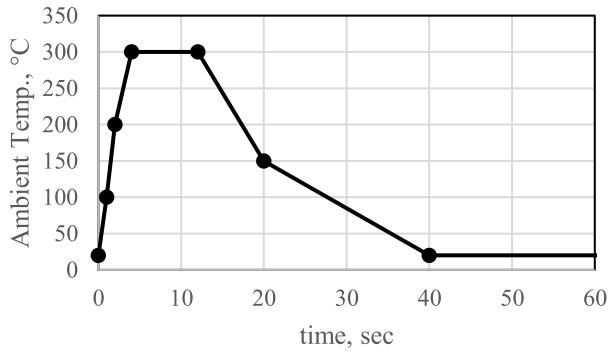

Figure 4: Temperature versus time used to describe the ambient temperature during gas quenching for the study.

Results and Discussion

Distortion from Common Gas Quenching Rates

Using the DANTE heat treatment simulation software, the Ferrium C64 disk was subjected to a range of possible HPGQ HTCs, using the time-temperature curve in Fig. 4. The following heat transfer coefficients were evaluated: 10, 25, 50, 100, 200, 300, 400, 500, 600, 700, 800, 900, and 1000 W/m^{2}K. Generally, HTCs of 200, 400, 700, and 1000 W/m^{2}K correspond to quench pressures of 2, 6, 10, and 20 bar, respectively. This relationship will vary depending on the flow pattern and velocity profile of the quench gas in the vessel and around the component.

The distortion mode of interest for this study was out-of-round of the eccentric bore. The distortion was determined by the difference of the distances B_1-B_2 and A_1-A_2, as shown in Fig. 5. Figure 6 shows the results from the study, plotted as out-of-round distortion, in µm, versus HTC, in W/m^{2}K.

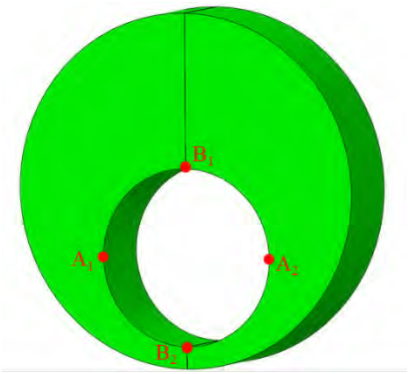

Figure 5: Points showing the locations of measurements defining the out-of-round distortion.

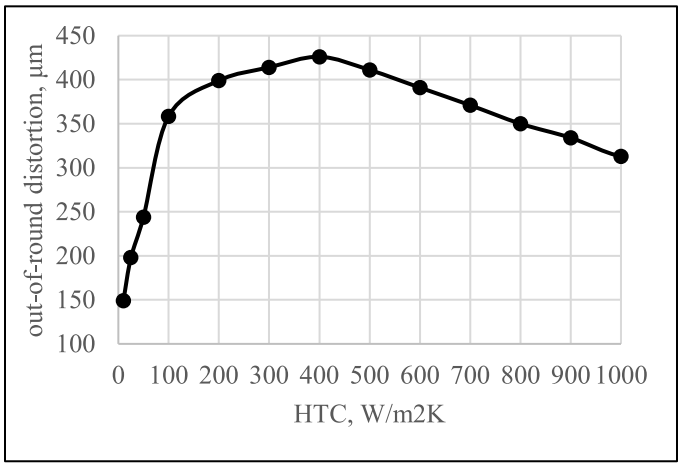

Figure 6: Out-of-round distortion of the coupon bore as a function of the heat transfer coefficient.

It is commonly assumed that if a component is quenched slower; i.e., a lower HTC value, less distortion will occur. As can be seen in Fig. 6, the highest HTC studied nearly produced the least amount of out-of-round distortion. The only HTCs that produced less distortion in this case can be associated with an air cool (10, 25, and 50 W/m^{2}K). The most distortion occurred from an HTC of 400 W/m^{2}K. This observation contradicts the above assumption and leads to the question: How can quenching slower produce more distortion?

Before answering that question, let's determine how the out-of-round distortion is introduced by examining the two critical process steps: Heating, during which time the initial microstructure is transformed to austenite, and cooling, during which time the austenite decomposes to martensite. During this study, the additional complexity introduced by the volume difference between the starting and ending microstructure is ignored by starting with a fully martensitic microstructure. Base carbon Ferrium C64, 0.1% carbon, will transform to martensite and a small amount of retained austenite if subjected to the HTCs examined in this study. Other materials may respond differently during quench due to transformation products other than martensite. Only Ferrium C64 was used for this study.

Distortion from Heating (Austenite Transformation)

The component starts with a fully martensitic microstructure at 20° C and is heated to 1000° C, transforming fully to austenite. The furnace starts at room temperature and is linearly ramped to 1000° C in 30 minutes. Figures 7 – 11 show the volume fraction of austenite (left) and radial displacement, in millimeters, of the bore (right) at critical times during the heating process. The radial displacement is with respect to the bore's geometric origin and all figures use a displacement magnification of 25X.

Figure 7 shows the component at the instant before austenite transformation starts. Due to the mass difference, the thin section of the bore heats faster, and is slightly larger in the radial direction, than the thick section of the bore. This makes the bore slightly larger in the vertical direction.

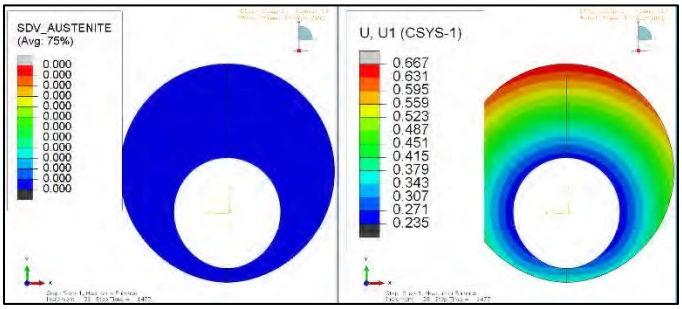

Figure 7: Snapshot of heating, just prior to austenite transformation, showing austenite phase fraction (left) and radial displacement of bore in mm (right).

Austenite transformation begins in the thinnest section first. The increase in density from martensite to austenite reduces the radial dimension at the thin section of the bore. This makes the bore slightly larger in the horizontal direction than in the vertical direction. As the austenite progresses up the sides of the bore, the increase in density begins to reduce the radial dimension around the bottom half of the bore. This increases the horizontal dimension of the bore even further, as shown in Fig. 8.

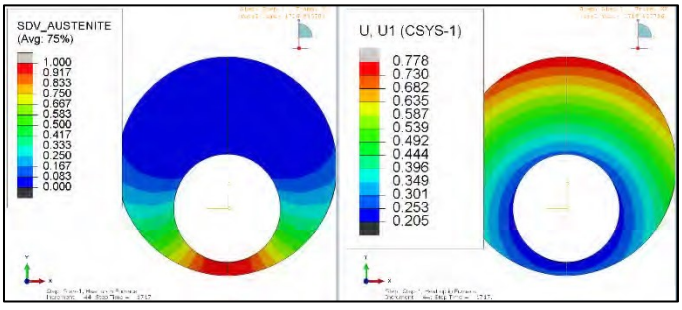

Figure 8: Snapshot during heating as the austenite progresses around the bore, showing austenite phase fraction (left) and radial displacement of bore in mm (right).

With the austenite transformation complete around the lower ¾ of the bore, the transformation in the thick section acts to stretch the bore vertically, as shown in Fig. 9. The stretching in the vertical direction is due to the shrinkage of the thick section.

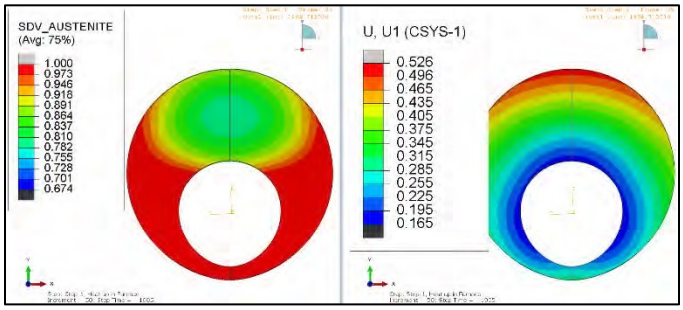

Figure 9: Snapshot during heating after the austenite has completed in thin section and is progressing through the thick section, showing austenite phase fraction (left) and radial displacement of bore in mm (right).

Since there is more mass to transform in the thick section, the bore is left stretched in the vertical direction after heating, as shown in Fig. 10.

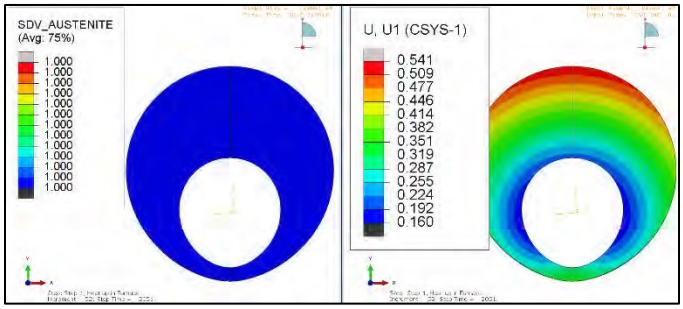

Figure 10: Snapshot at the end of the austenite transformation, showing austenite phase fraction (left) and radial displacement of bore in mm (right).

Once the component reaches 1000° C, there is an additional expansion, but the shape of the bore remains the same, as shown in Fig. 11.

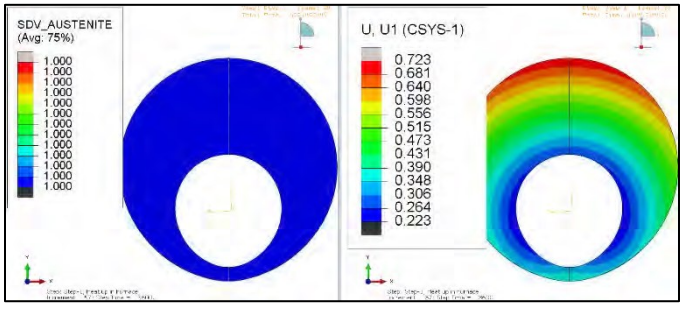

Figure 11: Snapshot at the end of heating, showing austenite phase fraction (left) and radial displacement of bore in mm (right).

The distortion generated from the heating process shown does not consider any residual stresses that may have been present from previous manufacturing operations, which would distort the component as the stresses are released from the high temperatures. The model also does not consider any thermal nonuniformities which may be present in the vessel. The part now proceeds to quench with a slightly out-of-round bore, even though precautions were taken to heat the part slowly and uniformly. The next section looks at the quenching process, and how the martensite transformation contributes to the out-of-round distortion.

Distortion from Quenching (Martensite Transformation)

Every HTC and ambient temperature combination will cause a slightly different distortion response, due to the timing of the martensite transformation in different locations of the part. However, the mechanism responsible for the out-of-round distortion remains the same. This example uses an HTC of 400 W/m^{2}K and the variable ambient temperature shown in Fig. 4 to demonstrate how the martensite transformation contributes to the out-of-round distortion of the bore. This example ignores the distortion from heating and instead assumes that the component starts at 1000° C, 100% austenite, and stress and strain free. Figures 12 – 17 show martensite phase fraction (left) and the radial displacement, in millimeters, of the eccentric bore (right) at several critical times during the quenching process. The radial displacement is relative to the bore's geometric origin and all figures use a displacement magnification of 25X.

Figure 12 shows the instance during quench just prior to the start of the martensite transformation. The bores vertical size has been significantly reduced by the thermal contraction of the thin section, while the thick sections remains relatively hot.

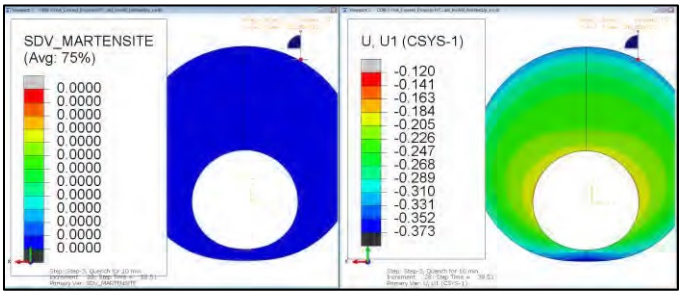

Figure 12: Snapshot of quenching, just prior to martensite transformation, showing martensite phase fraction (left) and radial displacement of bore in mm (right).

Figure 13 shows that ~85% martensite is now in the thin section and is beginning to progress from the bottom of the bore to the top. This initial transformation does not change the shape of the bore considerably, since the expansion of martensite from austenite acts to push in the horizontal direction. However, the bottom of the bore does grow a little wider during this initial transformation.

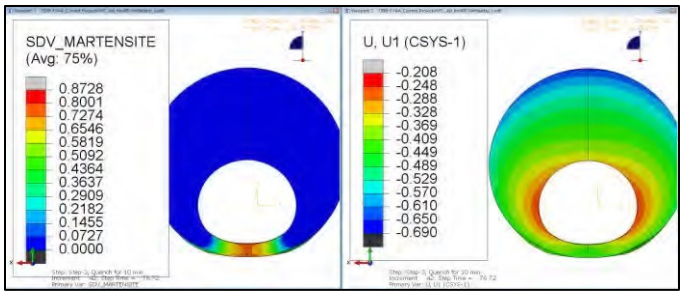

Figure 13: Snapshot during quenching as the martensite completes in the thin section and begins to progress around the bore, showing martensite phase fraction (left) and radial displacement of bore in mm (right).

As the martensite front progresses around the bore, the expansion acts to stretch the bottom of the bore in the vertical direction, as shown in Fig. 14. At this point, the radius at the bottom of the bore is smaller than the radius at the top of the bore.

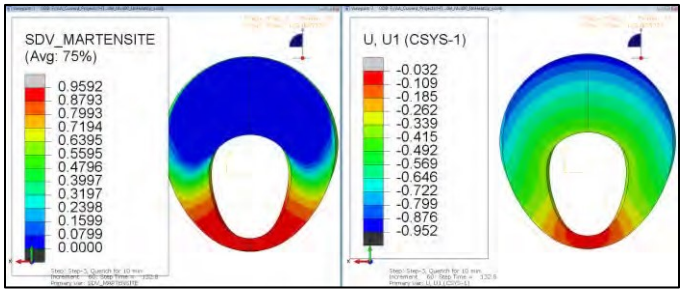

Figure 14: Snapshot during quenching as the martensite progresses around the bore, showing martensite phase fraction (left) and radial displacement of bore in mm (right).

With the martensite transformation complete in the lower half of the bore, and nearly complete on the upper half of the bore, the martensite transformation has significantly stretched the bore in the vertical direction, as shown in Fig. 15.

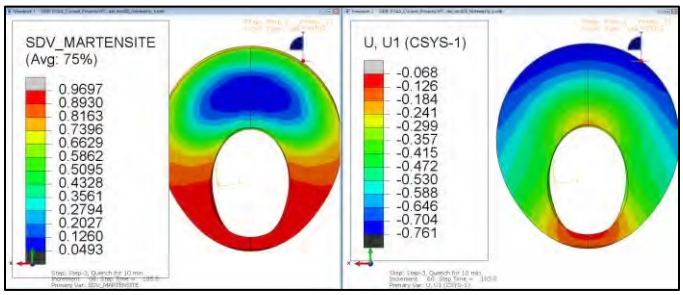

Figure 15: Snapshot during quenching after the martensite has completed in thin section and has begun around the top half of the bore. Shown is martensite phase fraction (left) and radial displacement of bore in mm (right).

As the martensite transformation begins to rapidly progress through the thick section, the reduction in density pushes the thick section out in the horizontal direction. This expansion reduces the oblong shape of the hole somewhat, but it is not enough to bring the bore back to a circular shape, as shown in Figure 16.

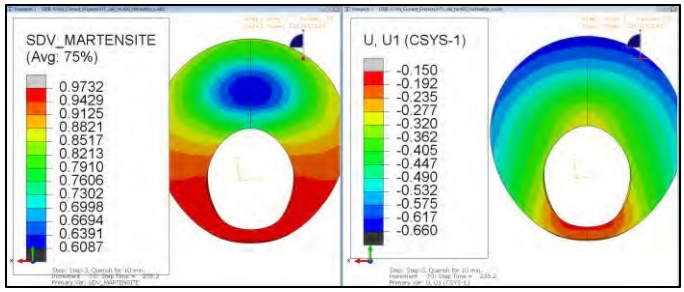

Figure 16: Snapshot during quenching after the martensite has completed in thin section, is nearly complete in the upper half of the bore, and is progressing rapidly through the thick section. Shown is martensite phase fraction (left) and radial displacement of bore in mm (right).

Once the martensite transformation is complete, ~97.5% for C64 with 0.1% carbon, the bore is clearly larger in the vertical direction, as shown in Fig. 17. The coupon is at room temperature in Fig. 17.

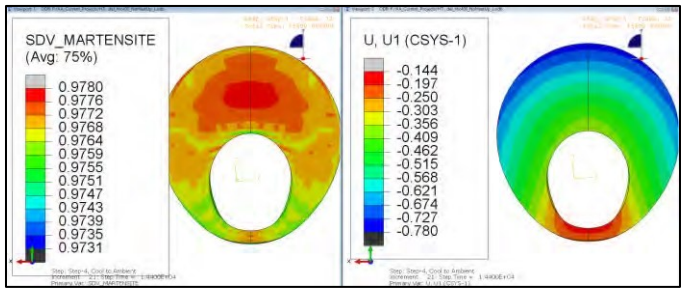

Figure 17: Snapshot at the end of quenching, showing martensite phase fraction (left) and radial displacement of bore in mm (right). The part is at room temperature at this point.

Armed with a better understanding of the mechanisms responsible for the out-of-round distortion of the bore, an examination of several conditions is needed to understand why a slower quench rate will not always lead to less distortion. The next section will compare three HTC values to explore this conundrum.

HTC Comparison

Referencing Fig. 6, since 100 W/m^{2}K (HTC100) produces more distortion than 1000 W/m^{2}K (HTC1000), but produces a significantly slower cooling rate in the component, these two conditions will be compared. These two conditions will also be compared to the HTC that causes the most out-of-round distortion of the bore, 400 W/m^{2}K (HTC400).

Table 2 outlines the out-of-round distortion for each of the three conditions caused by Heating Only, Quenching Only, and from the Entire Process. Also included is the sum of Heating Only and Quenching Only, compared to the distortion from the Entire Process. Since the heating was the same for all quenching HTCs, the difference in distortion must be from the quenching process. It should also be noted that the total out-of-round is the

sum of the distortion created by the heating and quenching processes for this particular geometry. Therefore, it is only necessary to examine the quenching process to determine what differentiates the three HTCs with respect to distortion of the bore.

Table 2: Comparison of Heating, Quenching, and Entire Process predicted distortion of bore for HTCs of 100, 400, and 1000 W/m^{2}K.

	HTC100 From Quenching	**HTC400 From Quenching**	**HTC1000 From Quenching**
out-of-round from Quenching	245.6 µm	319.1 µm	178.1 µm
	HTC100 From Heating	**HTC400 From Heating**	**HTC1000 From Heating**
out-of-round from Heating	135.6 µm	135.6 µm	135.6 µm
Sum of Quenching & Heating Distortion	381.2 µm	454.7 µm	313.7 µm
	HTC100 Complete Process	**HTC400 Complete Process**	**HTC1000 Complete Process**
out-of-round from Complete Process	358.5 µm	425.9 µm	313.3 µm
Percent Difference of Sum and Complete Process	6%	7%	0%

The out-of-round values reported in Table 2 include distortions from phase transformations and thermally induced plastic strain. Using the DANTE software, it is possible to disable the phase transformations during the analysis. Table 3 shows the out-of-round distortion of the bore for heating and quenching without the phase transformations to austenite and martensite, respectfully. The mechanical properties of austenite were used for the predictions reported in Table 3.

Table 3: Comparison of Thermally Induced predicted distortion of bore for HTCs of 100, 400, and 1000 W/m^{2}K.

	HTC 100 No Heat, No Phase	**HTC 400 No Heat, No Phase**	**HTC 1000 No Heat, No Phase**
out-of-round from Heating	5.8 µm	5.8 µm	5.8 µm
out-of-round from Cooling	25.5 µm	119.3 µm	112.6 µm

The thermally induced distortion from heating is very small, 5.8µm, due to the ramped heating. This small value can be considered insignificant and indicates that the nonuniform austenite transformation is responsible for the distortion during heating. The distortion caused by thermal effects during quenching, however, is very significant. The nonlinearity of the distortion with respect to the HTC is revealed without considering the phase change. However, HTC100 produces much less distortion than HTC1000. Whereas, when phase transformations are considered, HTC1000 results in the lowest predicted distortion. Therefore, to fully understand the distortion response of a component, the effects of phase transformations must be accounted for.

To determine how the highest HTC evaluated can produce less distortion than one of the lowest HTCs evaluated, a comparison between these three HTC values during the martensite transformation is warranted. Figures 19 – 23 show martensite phase fraction comparisons between the three HTC values: 100, 400, and 1000 W/m^{2}K. Figure 18 describes the two views shown in Figs. 19 – 23.

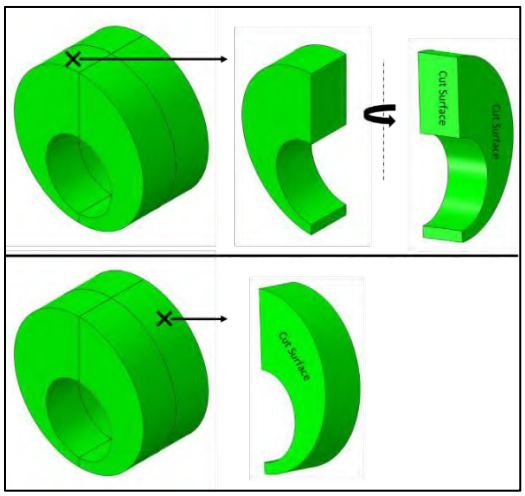

Figure 18: Description of views shown in Figures 19 – 23.

Each quarter section of the geometry will behave the same due to the geometric symmetry and the uniform HTC applied to all surfaces exposed to the atmosphere. The comparisons between the three HTC values are made when the maximum martensite phase fraction is approximately equal in particular sections of the coupon. The times at which these values occur will vary depending on the HTC value.

Figure 19 shows a comparison when the martensite phase reaches 80% for the first time. For all HTC values, this occurs on the outer edge of the thin section. At this snapshot in time, all three HTC values show a similar pattern. The maximum amount of martensite is at the thinnest section of the part on the surface of the end face. However, a few differences can be seen. Firstly, HTC100 has a significant amount of martensite, approximately 50%, already half way around the bore, with approximately equal amounts of martensite at the surface and in the core. Secondly, HTC400 also has an area of 50% martensite, but it is concentrated in the thin section of the coupon. The martensite fraction for HTC400, like HTC100, is almost equivalent on the surface and in the core. Thirdly, the HTC1000 martensite has progressed approximately the same distance around the bore as HTC400, but there is almost no martensite transformation occurring in the core at this time.

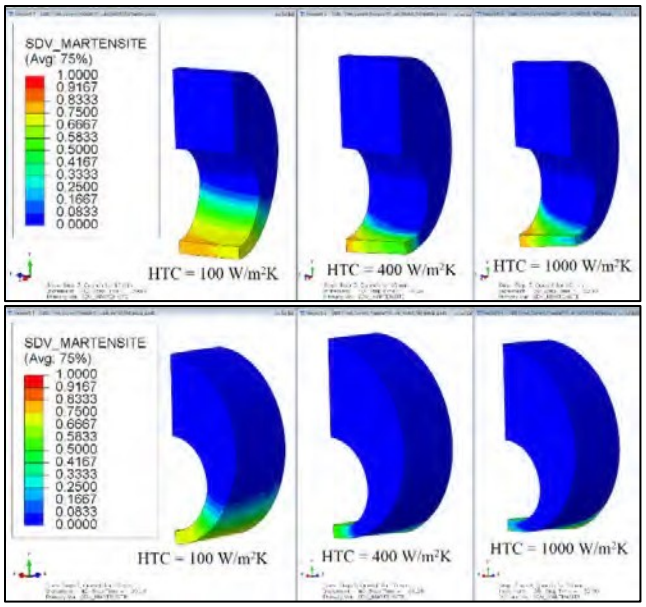

Figure 19: Comparison of martensite fraction for 3 HTC values when martensite fraction reaches 0.80.

It is ultimately this pattern, shown in Fig. 19, that is responsible for the variation in the distortion response of the eccentric bore. Figure 20 shows a snapshot when the martensite reaches 90% for each condition. It now becomes very clear that the martensite transformation for HTC100 progresses very uniformly from the surface to the core and is also very uniform over large volumes of material around the bore. The behavior of HTC400 is also becoming rather clear: The martensite transformation is very uniform from the surface to the core, just as HTC100. However, unlike HTC100, there is a relatively steep transformation gradient circumferentially around the bore.

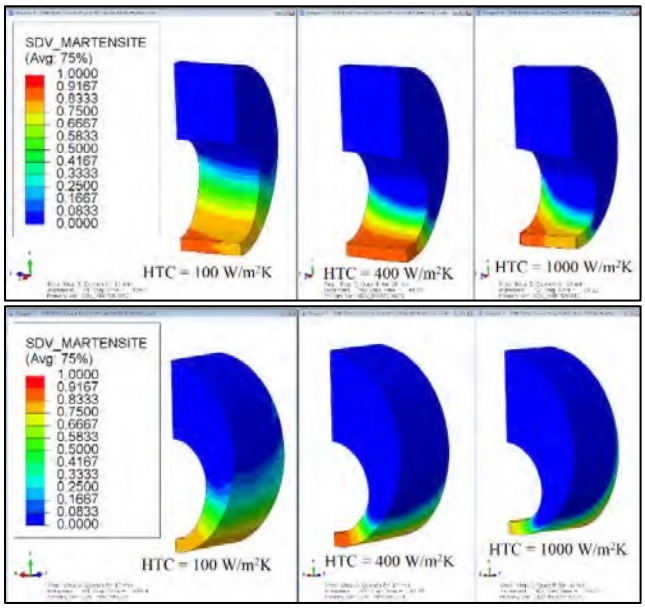

Figure 20: Comparison of martensite fraction for 3 HTC values when martensite fraction reaches 0.90.

As the martensite transformation progresses in HTC1000, reaching its maximum value of ~98%, there is a steep circumferential transformation gradient around the bore, as shown in Fig. 21. A steep transformation gradient also occurs from the surface towards the core, resulting in less martensite transformation per unit volume for HTC1000 than for HTC400. This phenomenon can be attributed to the reduced distortion of HTC1000. The bottom figure in Figure 21 clearly shows that the transformation is occurring on the surface of the thick section, even before the bore has completely transformed. This means that as the transformation progresses around the bore, acting to elongate the bore in the vertical direction, the transformation in the thick section is acting to offset this elongation by stretching the bore in the horizontal direction.

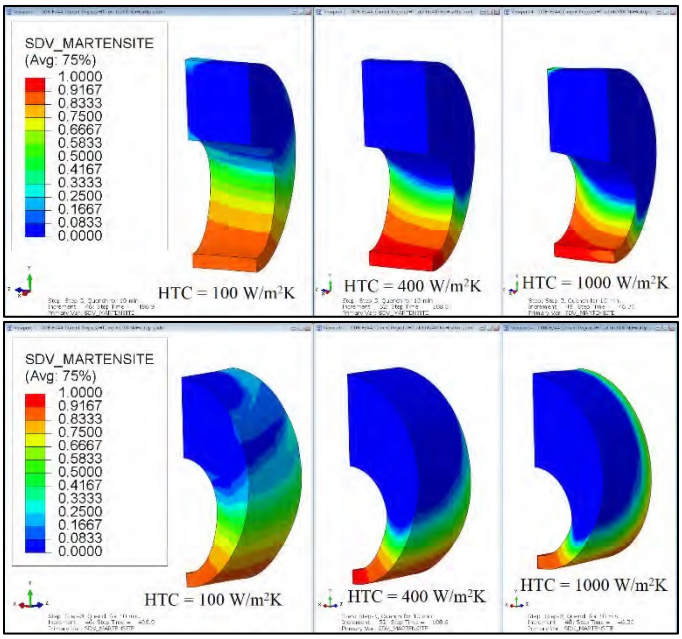

Figure 21: Comparison of martensite fraction for 3 HTC values when martensite fraction reaches ~0.98.

The next snapshot, Figure 22, shows the moment when the martensite transformation completes in the thin section of the coupon. It is now obvious as to why HTC400 produces the greatest amount of out-of-round distortion: A uniform transformation from the surface to the core, combined with a steep transformation gradient circumferentially around the bore, results in the bore being elongated in the vertical direction with no offsetting effect from transformations occurring in the thick section of the coupon. Although the transformation has started near the surface of the thick section of HTC400 in Fig. 22, the damage has already been done by the transformation completing in the thin section and nearly completing up the sides of the bore before starting in the thick section.

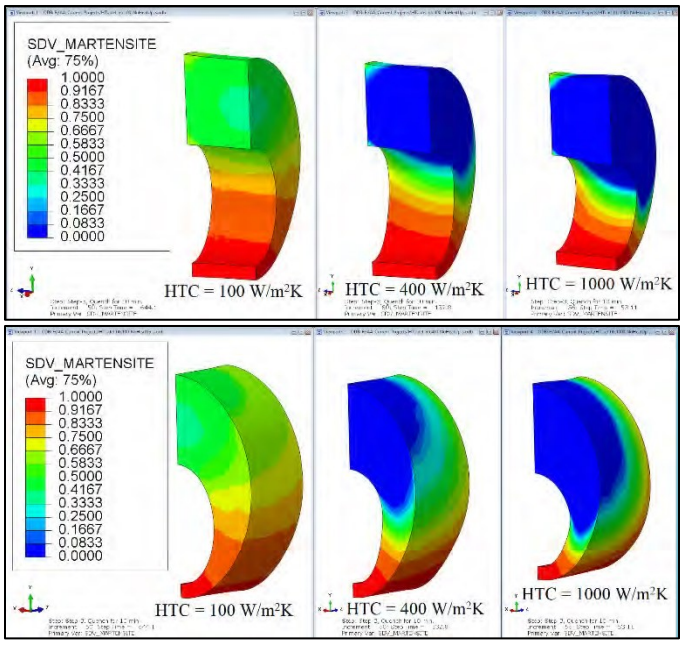

Figure 22: Comparison of martensite fraction for 3 HTC values when martensite fraction reaches 0.98 in thin section.

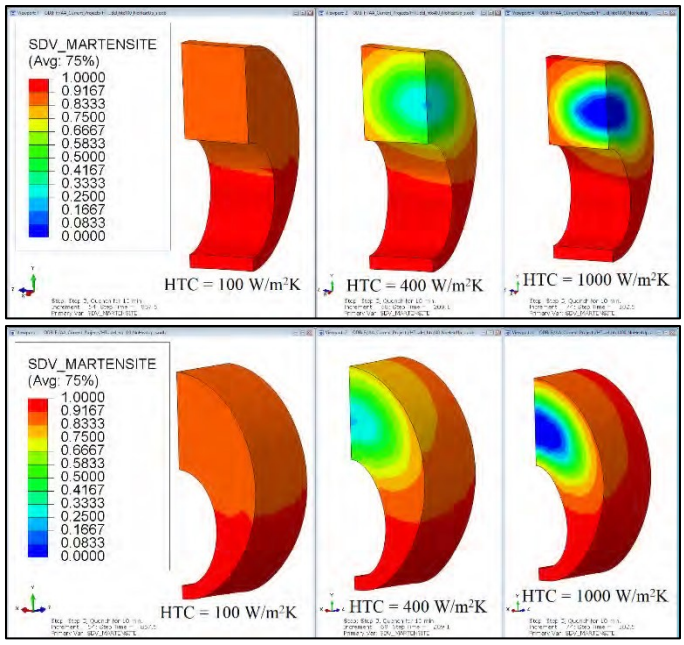

Figure 23: Comparison of martensite fraction for 3 HTC values when martensite fraction reaches 0.98 around all of bore.

The martensite transformation behavior from the HTC100 trial is in stark contrast to that of the HTC400 trial. The transformation for HTC100 progressed with a very shallow transformation gradient around the circumference of the bore, with the martensite beginning in the thick section well before the transformation was complete in the thin section. This allowed the elongating effect in the vertical direction, created by the martensite transformation progressing up the sides of the bore, to be offset by the stretching effect in the horizontal direction, created by the transformation to martensite in the thick section. Figure 22 shows that there is approximately 90% martensite halfway up the side the bore and nearly 60% martensite in the thick section of HTC100.

HTC1000's transformation around the bore progresses much like HTC400, but with one critical difference: As the martensite progresses up the sides of the bore, martensite is forming in the thick section. While Fig. 22. shows martensite in the thick section of HTC400 and HTC100, martensite in HTC400 only began forming after it had progressed a substantial amount around the bore. HTC1000, on the other hand, had martensite transforming in the thick section before it had progressed halfway around the bore in the core, as shown in Fig. 21.

Figure 23 shows the process as it is completing. It is worth noting the difference between HTC400 and HTC1000. HTC400 has a shallow gradient in the thick section from the surface to the core. This means there is a large amount of volume transforming in the thick section all at once, acting to stretch the hole in the horizontal direction, after the material around the bore had already transformed. HTC1000, on the other hand, has a steep transformation gradient and has much less material to transform before completion. This is due to the transformation in the thick and thin sections occurring simultaneously.

Additional Observations Concerning the Eccentric Bore

Due to differences in transformation timing at critical locations of the part, the distortion response did not behave as anticipated. The model presented used a simple geometry and a perfectly uniform heat transfer coefficient during heating and quenching. Reality is never this kind. In most cases the ambient temperature and/or the HTC in the bore would vary from the outer diameter and end faces of the coupon used in the study. Table 4 looks at five (5) scenarios of differing boundary conditions placed on the bore of HTC400, during quenching only, and compares them to the quench only HTC400 result. The ambient temperature profile and HTC from the above study were used for the outer diameter and end face surfaces of the coupon.

While gas quenching offers a more uniform method of heat extraction than liquid quenching, geometry can alter this uniformity. Generally, the ambient temperature in the bore of the geometry under study would be higher than other surfaces, due to radiant surfaces facing each other. The second and third rows of Table 4 show the out-of-round distortion results of the bore if the ambient temperature of the bore was 1.5 and 2 times higher than the outer diameter and end faces, respectively. The HTC is the same for all surfaces. The increase in ambient temperature essentially slows down the heat transfer through the bore wall and has a minimal effect on the total out-of-round distortion compared to the situation where the ambient temperature is the same for all surfaces.

A uniform HTC on all surfaces of this geometry is also highly unlikely in actual practice. There are two scenarios possible. First, air has a difficult time moving through the bore and the HTC in the bore is reduced compared to the other surfaces. The fourth row in Table 4 shows the results if the HTC in the bore is 0.5 times the HTC applied to other surfaces. Like the increased ambient temperature, this boundary condition acts to

slow the heat transfer through the bore wall and also has a minimal effect on the distortion compared to a uniform HTC. In the second scenario, a chimney effect is created through the bore and the HTC in the bore is higher than the other surfaces. This is quite common in actual practice. The last two rows in Table 4 show the out-of-round results if the HTC is 1.5 and 2 times greater than the HTC on other surfaces, respectively. The ambient temperature is the same for all surfaces. The increased HTC value acts to increase the heat transfer through the bore wall and reduces the out-of-round distortion of the bore compared to the uniform HTC.

Table 4: Comparison of predicted out-of-round distortion of bore for various boundary conditions on bore surface.

HTC400 Bore BC	
Condition	**Out-of-round, µm**
Uniform HTC and Equal Ambient Temperature	319
1.5X Ambient Temperature	313
2.0X Ambient Temperature	327
0.5X HTC	310
1.5X HTC	285
2.0X HTC	249

Another difficult to quench geometry is shown in the inset of Fig. 24. This geometry cools much faster on the side with the fins, due to the increased surface area provided by the fins. This geometry also has a nonlinear distortion response to uniform heat transfer coefficients in the range of HPGQ, as shown in Fig. 24. The distortion evaluated for this case was bow distortion of the coupon in the longitudinal direction. This is an example that shows that nonlinear responses to high pressure gas quenching is not unique to the geometry presented in the study but exists in most difficult to quench geometric features.

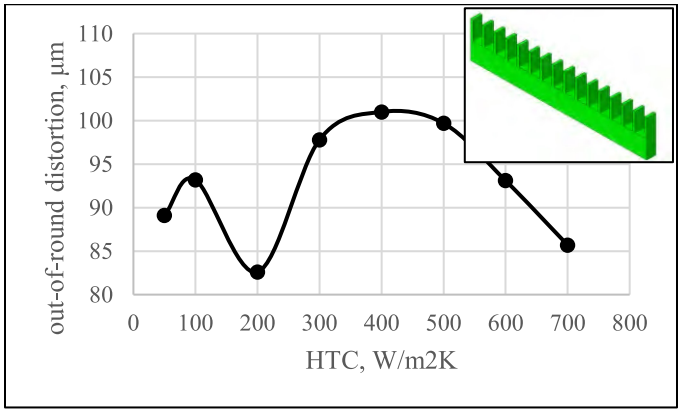

Figure 24: Predicted bow distortion of finned coupon, shown in the insert, as a function of the heat transfer coefficient.

Conclusions

From the study presented here, as well as from Table 4 and Fig. 24, it becomes clear that there is no easy way to determine a suitable gas pressure and velocity profile when turning to high pressure gas quenching to reduce distortion in difficult to quench geometries. While an understanding of the mechanisms responsible for particular distortion modes of certain geometric features is critical in the decision-making process, the ability to evaluate numerous conditions before any parts are processed should not be underestimated.

The out-of-round distortion, and any shape change distortion, is mainly due to the nonuniform, solid-state phase transformations, both to and from austenite, with the thermal effects having a marginal effect on the distortion. If nonuniformities cannot be avoided, due to geometric features, the slowest rate possible should not automatically be considered to result in the least amount of distortion. Finite element modeling of the heat treatment process, using software such as DANTE, can help the engineer choose the proper gas quenching process parameters to ensure mechanical properties are achieved while keeping distortion to an absolute minimum.

References

[1] V. Heuer, K. Loser, and D.R. Faron, “Low Distortion Heat Treatment of Transmission Components”, AGMA Technical Paper, October 2010.

[2] Tim Yu, Tony Yu, and D. Herring, “Low-Pressure Carburizing and High Pressure Gas Quenching”, *Heat Treating Progress,* September/October 2003, p 37-41.

[3] Z. Li, “Heat Treatment Response of Steel Fatigue Sample During Vacuum Carburization and High Pressure Gas Quenching Process”, *Proceedings of MSEC2015*, Charlotte, NC, June 2015.